Multi-slice Multi-echo Pulsed-gradient Spin-echo (MePGSE) Sequence for Diffusion Tensor Imaging MRI: A Preliminary Result

Geon-Ho Jahng*, Stephen Pickup†

*Department of Radiology, East West Neo Medical Center, Kyung Hee University College of Medicine, Seoul, Korea, †Department of Radiology, University of Pennsylvania Medical Center, Philadelphia, USA

An echo planar imaging (EPI)-based spin-echo sequence is often used to obtain diffusion tensor imaging (DTI) data on most of the clinical MRI systems. However, this sequence is confounded with the susceptibility artifacts, especially on the temporal lobe in the human brain. Therefore, the objective of this study was to design a pulse sequence that relatively immunizes the susceptibility artifacts, but can map diffusion tensor components in a single-shot mode. A multi-slice multi-echo pulsed-gradient spin-echo (MePGSE) sequence with eight echoes wasdeveloped with selective refocusing pulses for all slices to map the full tensor. The first seven echoes in the train were diffusion-weighted allowing for the observation of diffusion in several different directions in a single experiment and the last echo was for crusher of the residual magnetization. All components of diffusion tensor were measured by a single shot experiment. The sequence was applied in diffusive phantoms. The preliminary experimental verification of the sequence was illustrated by measuring the apparent diffusion coefficient (ADC) for tap water and by measuring diffusion tensor components for watermelon. The ADC values in the series of the water phantom were reliable. The MePGSE sequence, therefore, may be useful in human brain studies.

Key Words: MRI, Multi-slice multi-echo PGSE, Diffusion tensor imaging, Slice selective 180°

INTRODUCTION

Changes in self-diffusion have already proven to be significant with respect to pathology and have provided a new contrast mechanism in a medical imaging. Diffusion imaging techniques have found several applications in the studies of nerve tissue,[1] neurological disease,[2,3] and tumor.[4,5] The cell walls in living tissues represent semi-permeable barriers to water diffusion. Many tissues, therefore, exhibit diffusion anisotropy. Examples include white matter,[6] nerves,[1,7] and muscle[8] in which water diffusion is more rapid along the tissue fibers. The development of quantitative magnetic resonance imaging (MRI) measures of diffusion anisotropy could have important biological and clinical applications.

The accurate measurement of the full diffusion tensor is difficult to achieve in-vivo due to irregular bulk tissue motion. The bulk motion can easily overwhelm the microscopic incoherent molecular motions, leading to additional signal loss and an overestimation of the apparent diffusion coefficient (ADC), which is an only partial explanation of molecular motions. It is therefore desirable to acquire all data as rapidly as possible. The most commonly employed approach to minimization of errors due to motion is to apply the pulsed-gradient spin-echo (PGSE) sequence as a preparation of a fast imaging sequence.[9] In most cases, an echo planar imaging (EPI) sequence is used for image acquisitions.[10-12] However, the PGSE-EPI technique does have several limitations. For examples,the EPI technique suffers from a low signal-to-noise ratio, susceptibility artifacts, and low resolution.[11,12] Utilization of alternative imaging techniques that have reduced the limitations has been proposed for diffusion applications such as the projection reconstruction,[13]

This study was supported by a grant of the Korea Health 21 R&D Project, Ministry of Health & Welfare, Republic of Korea (A062284).
Submitted April 16, 2007, Accepted June 3, 2007
Corresponding Author: Geon-Ho Jahng, Department of Radiology, East West Neo Medical Center, 149, Sangil-dong, Gangdong-gu, Seoul 134-727, Korea.
Tel: 02)440-6187, Fax: 02)440-6932
Email: ghjahng@gmail.com

the BURST imaging,[14] and the line selective scan techniques.[15,16] The methods, however, require a specialized image processing and have unacceptably long acquisition times ina clinical study.

Multi-echo PGSE imaging sequences havebeen previously described for measuring diffusion.[17-19] Those methods made use of hard pulses or composite pulses for refocusing making the sequence suitable only for a single slice acquisition and significantly reducing the efficiency of the imaging acquisition. Hard pulses or composite pulses were used in the previous reports in order to minimize the artifacts due to incomplete refocusing of the magnetization.

The objective of this paper, therefore, was to develop a multi-slice multi-echo pulsed-gradient spin-echo (MePGSE) sequence for a diffusion tensor imaging. Each echo in the train wasdiffusion-weighted allowing for the observation of diffusion in several different directions in a single experiment. The exam time was thus reduced by a factor equal to the number of echoes in the train. Successful implementation of such a technique required considerations of all the artifacts due to the limitations of the frequency selective refocusing pulses. We implemented rewinding gradients on the phase encode, crusher gradients around the refocusing pulses, and a two-step phase cycling scheme with the half Fourier acquisition to minimize the artifacts. In addition, an additional refocusing pulse was implemented to minimize the residual magnetizations at the end of the pulse train. Images generated by the new sequences are presented and the resulting image quality is discussed.

MATERIALS AND METHODS

1. Multi-echo pulsed-gradient spin-echo (MePGSE) sequence

We developed a multi-echo PGSE (MePGSE) imaging sequence with diffusion-weighted gradients in a different direction on each echo. We used slice selective refocusing pulses with a single shot experiment for measurements of the whole diffusion tensor. The resulting sequence can therefore be run in multi-slice acquisition mode. We modified a conventional single-echo spin-echo sequence by adding the refocusing pulses, phase-encoding gradients, and the readout-encoding gradients. A schematic of the sequence was depicted in the Fig. 1. The pulse sequence was symmetric around the refocusing pulses with respect to all gradients in order to minimize artifacts. The delay between echoes was constant and as short as possible in order to minimize signal losses due to T_2 relaxation decay. Slice selective refocusing pulses of 2.56 msec duration were used throughout the sequence. The slice selective refocusing pulses were caused to generate unwanted signals. In order to minimize the unwanted signal, we implemented the following methods.

A rewinding gradient on the phase encode axis was used to suppress coherence artifacts (the mirror imaging ghost). In the Fig. 1, the arrows on the phase encode axis indicated the direction of phase encoding and rewinding gradients for each echo. The pattern of the encoding and rewinding gradients indicated in the figure was corrected for the phase inversion generated by the refocusing pulses and was required to produce images that had a consistent orientation.

Crusher gradients around the refocusing pulses were also

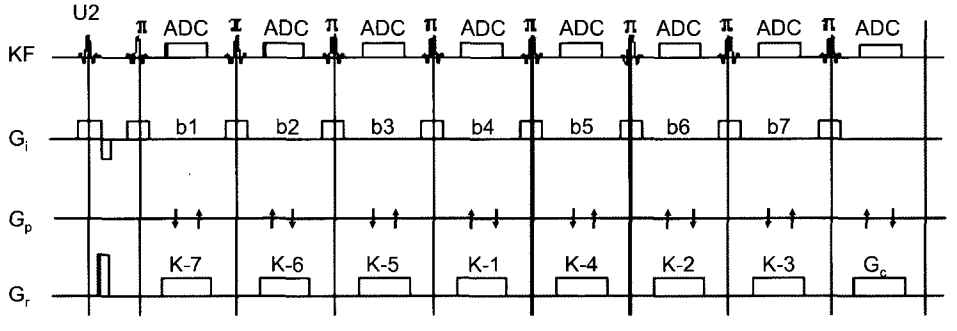

Fig. 1. A schematic drawing of the slice selective multi-echo pulsed-gradient spin-echo (MePGSE) sequence developed in the current study. Only the imaging gradients are shown in the figure. The labels in the figure indicated of which the different diffusion gradients was used for each echo.

employed to further suppress coherence artifacts with the amplitude of 2.0 mT/m, −2.0 mT/m, and 4.0 mT/m for the 1st, 2nd, and 3rd echoes, respectively. Crusher gradients were also applied at the end of the sequence in order to suppress residual magnetization artifacts. A two-step phase cycling scheme with the half Fourier acquisition was implemented for further suppression of artifacts.

The diffusion gradients were symmetric about the refocusing pulses and the diffusion time, Δ, was the same for all echoes. All diffusion gradients were used in trapezoidal envelopes with 0.72 msec of the ramp time. The amplitudes of all diffusion gradients in the sequence were identical. Such gradients may be applied on any of the three gradient axes simultaneously to achieve a maximum net gradient. The orientation of the diffusion gradient axis and its net magnitude was thus determined by which gradients were turned on for the given echo. Seven different gradient orientations[8] generated by combinations of the physical gradients were identified using the index k listed in the Table 1 and shown in the Fig. 1 to indicate the orientation of the diffusion-weighted index for each echo in the pulse train. Echoes with k=1, 2, 3, and 4 were used in all three gradients simultaneously, while echoes with k=5, 6, and 7 were used only a single gradient axis. The order of diffusion-weighted echoes was selected to reduce artifacts and to provide the best signal-to-noise ratio (SNR).

In this sequence it was necessary to minimize the echo time (TE) because of significant reductions of signal intensities in the later echoes. This minimization of the TE was conducted by increasing in the amplitude of the imaging gradients that ultimately limited the minimum field-of-view (FOV) and the slice thickness (TH). The best tradeoff between these conflicting requirements yielded the sequence with the minimum FOV=150 mm and TH=2 mm which was reasonable to scan the human brain. This sequence was run several times while the amplitude of the diffusion gradients was increased linearly on each measurement, but other parameters were held constant between consecutive runs of the sequence.

Table 1. The gradient orientations used in the current study. The k is the number of echoes and a_x, a_y, and a_z are the polarities of diffusion encoding gradients. ADC stands for the apparent diffusion coefficient. D_{av} is the average diffusion coefficient. D_{xy}, D_{xz}, and D_{yz} are the three off-diagonal diffusion coefficients and D_{xx}, D_{yy}, and D_{zz} are the three diagonal diffusion coefficients of the diffusion tensor.

k	a_x	a_y	a_z	G_{net}	ADC (D^k)
1	+1	+1	+1	$\sqrt{3}\ G_0$	$D_{av}+(2/3)(D_{xy}+D_{xz}+D_{yz})$
2	+1	−1	−1	$\sqrt{3}\ G_0$	$D_{av}+(2/3)(-D_{xy}-D_{xz}+D_{yz})$
3	−1	−1	+1	$\sqrt{3}\ G_0$	$D_{av}+(2/3)(D_{xy}-D_{xz}-D_{yz})$
4	+1	−1	+1	$\sqrt{3}\ G_0$	$D_{av}+(2/3)(-D_{xy}+D_{xz}-D_{yz})$
5	+1	0	0	G_0	D_{xx}
6	0	+1	0	G_0	D_{yy}
7	0	0	+1	G_0	D_{zz}

2. Experiments and data processing

Experiments were carried out using a 1.5 T whole body MR system (Magnetom Vision, Siemens, AG, Erlangen) with a head circular polarization coil. The gradient system was capable of producing the gradient amplitude of up to 25 mT/m with the rise time as short as 25 microseconds per mT/m. The gradient vectors to obtain full diffusion tensor were listed in Table 1. The relationship between the ADC and the tensor elements was also listed in the table for each gradient vector.

The MePGSE experiments were conducted on a water phantom and a watermelon to verify the sequence with measuring apparent diffusion coefficients. The waterphantom was constructed out of a plastic container containing tap water. The experiments were conducted at the room temperature of 21.5°C. The measurement parameters were the repetition time (TR)=2.0 sec, TE_n=50*n msec where n was the number of echo, the matrix size=128×128 with half Fourier (HF), FOV=180 mm, the number of acquisition (NA)=2 per phase encoding step, and TH=10 mm. Total scan time was 4 min 34 sec for each run of the sequence. Seven measurements were performed with gradient amplitudes ranging from 3 to 21 mT/m. An evaluation of the gradients in the MePGSE sequence revealed that the contribution of the gradient ramps was less than 0.1%. Therefore, the gradient ramps were ignored in the b-value calculations. The duration of diffusion gradientand the diffusion time were δ=10.70 msec and Δ= 30.42 msec, respectively. The b values were evaluated with considering effects of diffusion and imaging gradients derived by Li and Sotak.[18] Maps of the elements of diffusion tensor were calculated for each slice on a pixel-by-pixel basis from the slop of a linear least-mean-squares fit of the natural

logarithm of the signal intensity ratio to the *b*-values. The MATLAB program (The MathWorks, Inc., Natick, Massachusetts) was used for evaluating *b*-values, elements of the diffusion tensor, and eigenvalues of the diffusion tensor.

RESULTS

The result of the water phantom study was summarized in the Table 2. The calculated b-values were between 300 and 800 sec/cm^2 for the smallest diffusion gradient (3.0 mT/m) and were between 1,000 and 30,100 sec/cm^2 for the largest diffusion gradient (21.0 mT/m). The contributions of imaging gradients to the *b*-values were also listed in the table presented as the percentage of the lowest amplitude of the diffusion gradient. The cross-talk in the slice direction wasfound to be much smaller than in the readout direction because the duration and amplitudes of the slice selection gradients were considerably smaller. This contribution was significant at low gradient amplitudes and leaded to inaccuracies in measured ADC if not included in the analysis.

The average signal intensity in a region near the center of the images was measured for each image. The logarithm of the ratio of the intensity of images generated on consecutive echoes was then plotted as a function of the *b*-values shown in the Fig. 2. In the figure the vertical axis was the ratio of signal intensities and the horizontal axis was the *b*-values. The solid lines in the figure were the result of the least square linear fit of experimental data.

The ADCs andthe residuals generated by the least square analysis were listed in the last two rows of the Table 2. With the exception of the third echo, the fits were quite good as indicated by the residuals. In an isotropic medium, the ADC should be independent of direction. However, measured ADC shows substantial variability between the echoes. This study was repeated several times in order to determine if this was due to a systematic error. The values listed in the table were found to be highly reproducible.

We also tested a watermelon which has some internal

Table 2. Summaries of the measured and calculated parameters used for measurements of apparent diffusion coefficients on the water phantom.

Echo #	1	2	3	4	5	6	7
Δb (%)[a]	42	12	11	20	19	-20	19
ADC[b]	2.21	1.96	1.89	2.02	2.10	2.12	2.30
R^2	0.99	0.99	0.97	0.99	0.99	0.99	0.99

[a]Contributions of imaging gradients in the percentage to the b-value calculated with the gradient amplitude of 3.0 mT/m. [b]ADC: apparent diffusion coefficient with units of 10^{-5} cm^2/sec. R^2 is the result of the least square linear fit of experimental data.

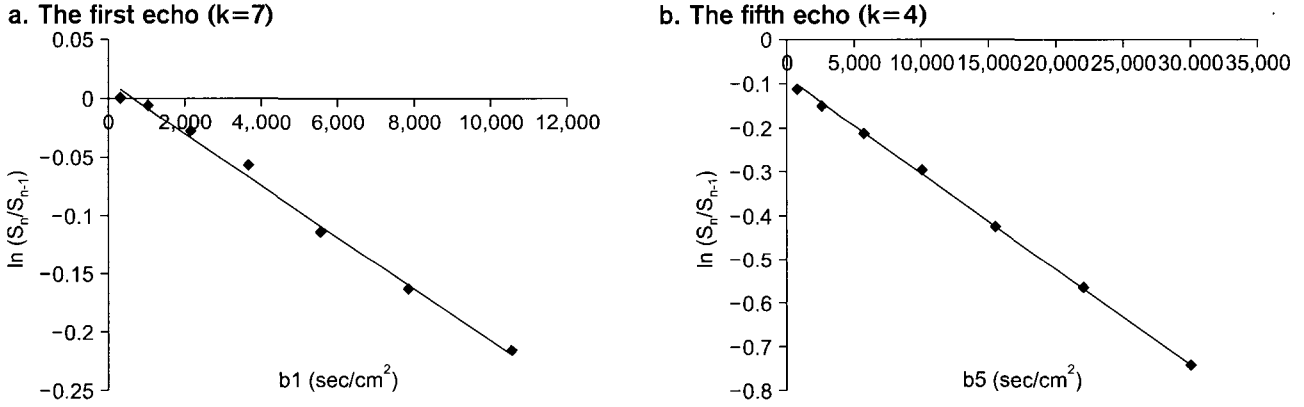

Fig. 2. Semi-logarithmic plots of the ratio of the average intensity from consecutive echoes versus the *b*-value for two representativeechoes (the first echo of Fig. 2a and the fifth echo of Fig. 2b) obtained from the water phantom study. The solid line represents the result of the least square linear fit of experimental data.

structures. The TE in the present study was reduced to 40 msec to provide improved signal-to-noise ratios in the later echo images. It was necessary to increase the amplitudes of diffusion gradients in order to achieve this reduction in TE. The diffusion gradient parameters were δ=10.7 msec and Δ =20.42 msec. All other parameters were identical to the previous study. The *b*-values were between 150 and 500 sec/cm^2 for 3.0 mT/m of the diffusion gradient. The *b*-values for 21.0 mT/m of the diffusion gradient were between 6,200 and 19,000 sec/cm^2. The average signal intensity of a homogeneous area in the watermelon was measured in each of the images. These data were then evaluated in the same manner as was done for the water phantom. The resulting average ADCs were between 1.16×10^{-5} and 1.94×10^{-5} cm^2/sec. The surface ADC value of the watermelon, however, could differ to the center ADC value because the temperature distributes through the watermelon.

The targeted application for the MePGSE sequence was to generate images of components of the diffusion tensor. The elements of the diffusion tensor were then calculated for each pixel. Images of some of the diffusion tensor elements were depicted in Fig. 3. Similar images were generated for the remaining elements of the diffusion tensor. Note that the intensity of the image for the off-diagonal term has relatively the low signal intensity. This suggests the diffusion in the watermelon is nearly isotropy.

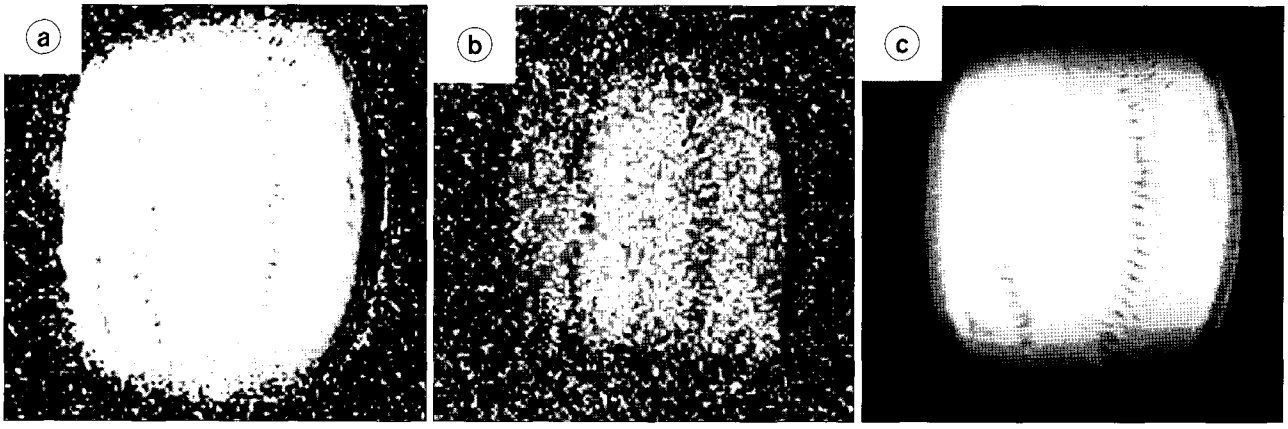

Fig. 3. Representative maps of the two diffusion tensor components obtained from the watermelon study. D_{yy} (a) and D_{yz} (b) are diffusion tensor maps represented on a diagonal component and an off-diagonal component, respectively and the structure image (c) of the same slice is also shown for the reference.

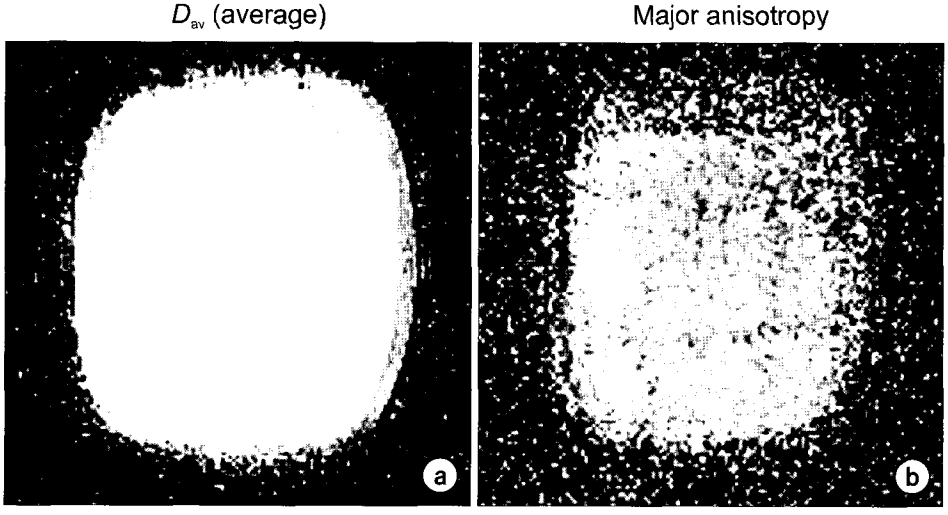

Fig. 4. Images of the isotropic (a) and major anisotropic (b) components of diffusion in watermelon.

Images of the principle components of the diffusion tensor were also generated by diagonalization of the diffusion tensor for each pixel. These results were then used to calculate the isotropic and major anisotropic components of diffusion shown in Fig. 4. Note that the signal-to-noise ratio in the image of the major component of the diffusion anisotropy is very poor since the watermelon is again nearly isotropic diffusivity.

DISCUSSION AND CONCLUSION

A multiple echo sequence was implemented in which the diffusion tensor can be collected in a single-shot manner. The multiple echo technique provideda significant reduction in the acquisition time compared to a single echo technique. The sequence developed in the present study was utilized in slice selective refocusing pulses thereby allowing it to operate in multi-slice mode.

Coherence artifacts are particularly problematic in a multi-echo imaging sequence such as the one proposed here. Several approaches to suppression of unwanted echoes were incorporated into the proposed sequence. Numerically optimized excitation and refocusing pulses were used throughout the sequence. The response profiles of the excitation/refocusing pulse pair were matched in order to reduce the amount of magnetization that did not see the optimum flip angle. Crusher gradients were also implemented around each of the refocusing pulses in the sequence.[20] A phase rewinding technique was used to eliminate mirror image ghosts generated by stimulated echoes.[21] A two-step phase cycling technique was also used to further suppress coherence artifacts.[22]

On the water phantom study, most of the fits were quite good. However some divergences from linearity at low *b*-values were apparent in some of the plots. This was attributed to the contributions of unwanted echoes to the measured signal intensity. The first echo hadno interference from unwanted echoes and therefore provided the most accurate measurement of the ADC. The ADC generated by the first echo in the series was very reliable and was in close agreement with the literature.[23]

In addition, data obtained the first four echoes which were utilized all three gradient axes simultaneously were also appeared to be quite reliable. The larger diffusion gradients applied on all three axes may suppress the spurious echoes. Use of all three gradients simultaneously gave a $\sqrt{3}$ increase in the gradient strength. However, significant systematic errors in the measured ADC were apparent in the remaining echoes. These errors may be attributed to contributions from spurious echoes. The contribution of spurious echoes was increased with increasing the echo number until a dynamic equilibrium was formed. These unwanted echoes added to the measured signal intensity thereby resulting in a slower echo decay rate and an under-estimation of the ADC.

Nowadays, an EPI acquisition with a phase-array coil is popularly used to obtain DTI-MRI data. This technique provides anisotropic indexes of diffusion tensor with minimizing motion artifacts and reducing some susceptibility artifacts. However, some regions in the human brain such as the temporal lobe may still have a difficulty to apply this technique because of high susceptibility artifacts. To minimize the susceptibility artifacts, a non-EPI type technique such as a turbo spin-echo sequence may be another option to obtain the diffusion tensor. However, there are limitations in applications on a high magnetic field MRI system which is currently developing fast. One of the major limitations is high depositions of heat. Therefore, the proposed method may be inapplicable to a high field MRI system.

In conclusion, we developed a multi-slice multi-echo sequence that could be useful to apply on regions that have a lot of susceptibility artifactsto measure the diffusion tensor. All tensor components can be obtained with a single shot mode and the measured ADC was reliable.

REFERENCES

1. **Beaulieu C, Allen PS**: An in vitro evaluation of the effects of local magnetic-susceptibility-induced gradients on anisotropic water diffusion in nerve. Magn Reson Med 36:39-44 (1996)
2. **Zhang Y, Schuff N, Jahng GH, et al**: Diffusion tensor imaging of cingulum fibers in mild cognitive impairment and Alzheimer disease. Neurology 68:13-19 (2007)
3. **O'Sullivan M, Morris RG, Huckstep B, et al**: Diffusion tensor MRI correlates with executive dysfunction in patients with ischaemic leukoaraiosis. J Neurol Neurosurg Psychiatry 75:441-447 (2004)
4. **Moffat BA, Chenevert TL, Lawrence TS, et al**: Functional diffusion map: a noninvasive MRI biomarker for early stratification of clinical brain tumor response. Proc Natl Acad Sci

USA 102:5524-5529 (2005)
5. **Dorenbeck U, Butz B, Schlaier J, et al**: Diffusion- weighted echo-planar MRI of the brain with calculated ADCs: a useful tool in the differential diagnosis of tumor necrosis from abscess? J Neuroimaging 13:330-338 (2003)
6. **Pierpaoli C, Basser PJ**: Toward a quantitative assessment of diffusion anisotropy. Magn Reson Med 36:893-906 (1996)
7. **Stanisz GJ, Szafer A, Wright GA, Henkelman RM**: An analytical model of restricted diffusion in bovine optic nerve. Magn Reson Med 37:103-111 (1997)
8. **Conturo TE, McKinstry RC, Akbudak E, Robinson BH**: Encoding of anisotropic diffusion with tetrahedral gradients: a general mathematical diffusion formalism and experimental results. Magn Reson Med 35:399-412 (1996)
9. **Stejskal EO**: Use of spin echoes in a pulsed magnetic-field gradient to study anisotropic, restricted diffusion and flow. J Chemical Physics 43:3597-3603 (1965)
10. **Song AW, Wong EC, Tan SG, Hyde JS**: Diffusion weighted fMRI at 1.5 T. Magn Reson Med 35:155-158 (1996)
11. **Wong EC, Cox RW, Song AW**: Optimized isotropic diffusion weighting. Magn Reson Med 34:139-143 (1995)
12. **Turner R, Le Bihan D, Chesnick AS**: Echo-planar imaging of diffusion and perfusion. Magn Reson Med 19:247-253 (1991)
13. **Jakob PM, Kober F, Haase A**: Radial BURST imaging. Magn Reson Med 36:557-561 (1996)
14. **Doran SJ, Jakob P, Decorps M**: Rapid repetition of the "burst" sequence: the role of diffusion and consequences for imaging. Magn Reson Med 35:547-553 (1996)
15. **Gudbjartsson H, Maier SE, Mulkern RV, et al**: Line scan diffusion imaging. Magn Reson Med 36:509-519 (1996)
16. **Gudbjartsson H, Maier SE, Jolesz FA**: Double line scan diffusion imaging. Magn Reson Med 38:101-109 (1997)
17. **Sigmund EE, Song YQ**: Multiple echo diffusion tensor acquisition technique.Magn Reson Imaging 24:7-18 (2006)
18. **Li L, Sotak CH**: Diffusion measurements by pulsed field-gradient multiple spin echoes. J Magn Reson 92:411-420 (1991)
19. **Gulani V, Iwamoto GA, Jiang H, et al**: A multiple echo pulse sequence for diffusion tensor imaging and its application in excised rat spinal cords. Magn Reson Med 38:868-873 (1997)
20. **Barker GJ, Tofts PS**: Semiautomated quality assurance for quantitative magnetic resonance imaging. Magn Reson Imaging 10:585-595 (1992)
21. **Zur Y, Zou X, Neuringer LJ**: Multiecho, spin-echo sequence to eliminate unwanted echoes. Magn Reson Med 19:464-469 (1991)
22. **Zur Y, Stokar S**: A phase-cycling technique for canceling spurious echoes in NMR imaging. J Magn Reson 71:212-228 (1987)
23. **Stejskal EO, Tanner JE**: Spin Diffusion Measurements: Spin Echoes in the Presence of a Time-Dependent Field Gradient. J Chem Phys 42:288-292 (1964)

일회 영상으로 확산텐서 자기공명영상을 얻을 수 있는 다편-다에코 펄스 경사자장 스핀에코(MePGSE) 시퀀스의 초기 결과

*경희대학교 의과대학 동서신의학병원 영상의학교실, †미국 펜실바니아대학병원 영상의학과

장 건 호* · Stephen Pickup†

대부분의 임상용 자기공명영상 장치에서 확산텐서(diffusion tensor) 영상을 얻기 위하여 에코플렌(EPI) 스핀에코(spin-echo) 시퀀스를 사용한다. 하지만 이 영상법은 자화감수성에 매우 예민한 단점이 있다. 따라서 본 연구의 목적은 자화감수성에 의해 발생하는 영상의 변질을 최소화하면서 확산텐서를 한번에 얻을 수 있는 시퀀스를 개발하는데 있다. 모든 확산 텐서 성분을 한번에 얻기 위하여 다편(multi-slice) 8에코 스핀에코 시퀀스(MePGSE)가 개발되었다. 모든 180도 펄스는 기존에 사용된 방법과는 달리 선택된(slice selective) 경사자장을 이용하였다. 처음 7개의 에코 영상은 확산텐서 영상을 위하여 사용하였고, 마지막 에코 영상에서는 영상을 얻는 경사자장은 사용하지 않고 남아있는 자화를(residual magnetization) 최소화하기 위하여 삼차원 경사자장(crusher gradients)만을 사용하였다. 따라서 6개의 텐서 성분을 단 한번의 실험에 의하여 얻을 수 있었다. 이 시퀀스를 사용하여 물과 수박을 이용하여 실험을 하였으며 물에서의 확산 값이 기존에 출판된 값과 유사하게 나타나 본 연구에서 MePGSE 시퀀스의 신뢰를 가질 수 있었다.

중심단어: 자기공명영상; 다편다에고 PGSE, 확산텐서 영상, 슬라이스 선택된 180 펄스